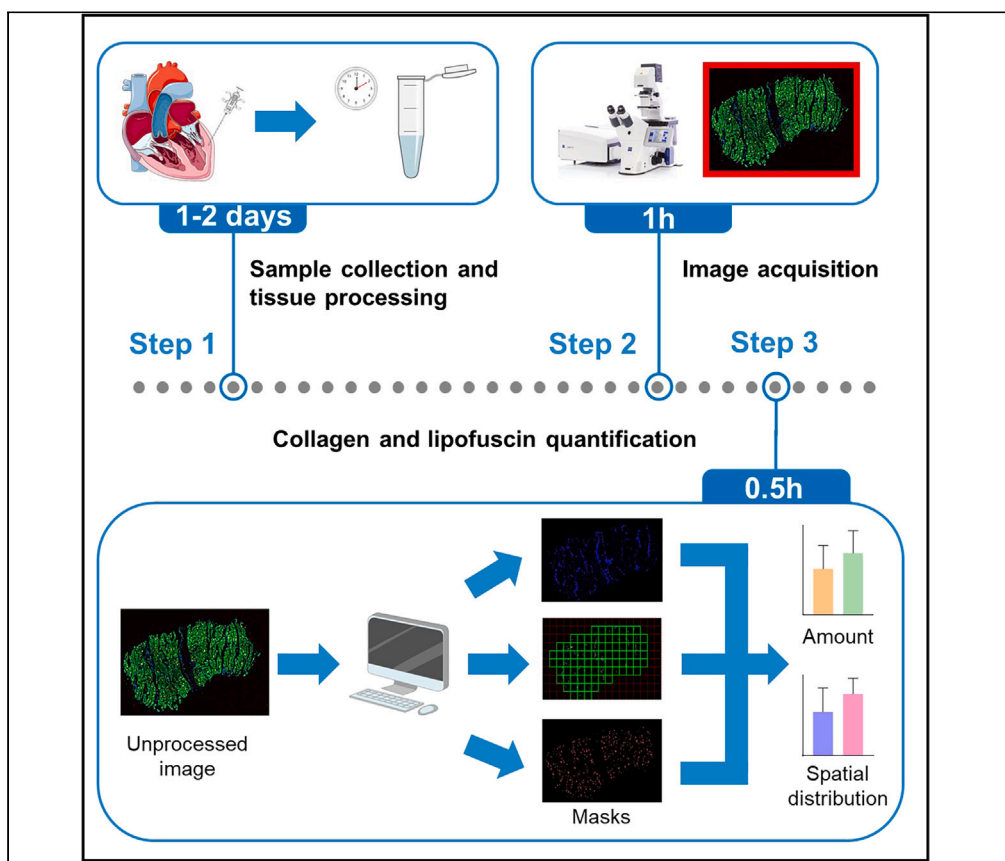


Protocol

Automatic quantification of myocardial remodeling features in human ventricular tissue from label-free microscopy



Laura García-Mendivil, María Pérez-Zabalza, Sam Duwé, Laura Ordoñas, Esther Pueyo

lgmendivil@unizar.es (L.G.-M.)
 mariapzabalza@unizar.es (M.P.-Z.)
 lordovas@unizar.es (L.O.)

Highlights
 Protocol for label-free microscopy image acquisition from ventricular tissues

Pipeline for automated collagen and lipofuscin amount and spatial distribution analysis

Applicable to other fibrotic tissues from any species

The procedures used routinely for collagen and lipofuscin evaluation are, in many cases, qualitative, observer dependent, and disregard spatial distribution. Here, we present a protocol for automatic quantification and spatial characterization of collagen and lipofuscin from label-free microscopy images of human ventricular tissues. We describe the steps for sample collection, tissue processing, image acquisition, and quantification of collagen and lipofuscin. This protocol avoids discrepancies between observers and can be adapted to other tissues and species.

Publisher's note: Undertaking any experimental protocol requires adherence to local institutional guidelines for laboratory safety and ethics.

García-Mendivil et al., STAR Protocols 4, 102730
 December 15, 2023 © 2023 The Authors.
<https://doi.org/10.1016/j.xpro.2023.102730>



Protocol

Automatic quantification of myocardial remodeling features in human ventricular tissue from label-free microscopy

Laura García-Mendivil,^{1,2,7,8,*} María Pérez-Zabalza,^{1,2,3,7,*} Sam Duwé,⁴ Laura Ordovás,^{1,2,5,9,*} and Esther Pueyo^{1,2,6}

¹Biomedical Signal Interpretation and Computational Simulation Group (BSICoS), Aragón Institute of Engineering Research, University of Zaragoza, 50018 Zaragoza, Spain

²BSICoS, Instituto de Investigación Sanitaria Aragón (IISA), 50018 Zaragoza, Spain

³Defense University Centre (CUD), 50090 Zaragoza, Spain

⁴Advanced Optical Microscopy Centre, Biomedical Research Institute, Hasselt University, 3500 Diepenbeek, Belgium

⁵Fundación Agencia Aragonesa para la Investigación y el Desarrollo (ARAID), 50018 Zaragoza, Spain

⁶Biomedical Research Networking Center in Bioengineering, Biomaterials and Nanomedicine (CIBER-BBN), 50018 Zaragoza, Spain

⁷These authors contributed equally

⁸Technical contact

⁹Lead contact

*Correspondence: lgmendivil@unizar.es (L.G.-M.), mariapzabalza@unizar.es (M.P.-Z.), lordovas@unizar.es (L.O.)
<https://doi.org/10.1016/j.xpro.2023.102730>

SUMMARY

The procedures used routinely for collagen and lipofuscin evaluation are, in many cases, qualitative, observer dependent, and disregard spatial distribution. Here, we present a protocol for automatic quantification and spatial characterization of collagen and lipofuscin from label-free microscopy images of human ventricular tissues. We describe the steps for sample collection, tissue processing, image acquisition, and quantification of collagen and lipofuscin. This protocol avoids discrepancies between observers and can be adapted to other tissues and species. For complete details on the use and execution of this protocol, please refer to García-Mendivil et al. (2022).¹

BEFORE YOU BEGIN

We outline a step-by-step automatic image acquisition and processing protocol for quantification of the amount of lipofuscin and for the analysis of collagen content, aggregation and spatial distribution in human left ventricular tissue samples. The availability of high-quality images is assumed. Data acquisition is performed on a Zeiss LSM880 microscope (Carl Zeiss, Germany) equipped with components for nonlinear optical (NLO) imaging but can be performed using any high-end confocal microscope equipped for NLO imaging. Even if our protocol is optimized for images of confocal microscopy, it could potentially be applied to wide-field fluorescent images as long as the resolution is sufficiently high. There is no limit on the number of images that can be analyzed using this approach.

Institutional permissions

Collection and analysis of human left ventricular samples conformed to the principles outlined in the Declaration of Helsinki and were approved by the local ethics committee (CEICA, reference number P117/0023), with all patients giving written informed consent before surgery and prior to their inclusion in the study.



For future applications of our described protocol, all procedures involving collection and processing of human samples must be approved by the relevant Ethics Committee.

KEY RESOURCES TABLE

REAGENT or RESOURCE	SOURCE	IDENTIFIER
Chemicals, peptides, and recombinant proteins		
Paraformaldehyde solution 4% in PBS	Biogen Cientifica	sc-281692
Sodium azide	Merck Life Science	71289-5G
PBS, without calcium, without magnesium	Biowest	L0616-500
Paraffin	E11K7052	Sakura Finetek Spain
Software and algorithms		
Zen Blue 2.5	Carl Zeiss GmbH	https://www.zeiss.com/microscopy/int/products/microscope-software/zen.html
Zen Black (ZEN 2.3 SP1 FP3)	Carl Zeiss GmbH	https://www.zeiss.com/microscopy/int/products/microscope-software/zen.html
ImageJ 1.53k	NIH	https://imagej.net/
MATLAB 2020b	MathWorks	https://es.mathworks.com/products/matlab.html
Experimental models: Organisms/strains		
Human	Age and gender data are published in García-Mendivil et al. ¹	

STEP-BY-STEP METHOD DETAILS

This protocol includes the following steps: sample collection, image acquisition, image pre-processing, analysis of collagen amount, aggregation and spatial distribution and lipofuscin quantification.

Sample collection

⌚ **Timing:** 1–2 days for tissue collection and fixation and 1 day for tissue sectioning

This section describes the procedure used for tissue collection and processing before image acquisition.

1. Collect left ventricular tissue samples from donors immediately after being placed on cardiopulmonary bypass. Specifically, transmural biopsies can be extracted using a 14G tru-cut needle without perforating the myocardial wall.

Note: Transmural left ventricular tissue samples obtained from living donors are used in this protocol, but other kinds of tissues discarded for transplantation, endocardial biopsies, or cadaveric tissues could be used too.

2. Store the tissue samples in ice-cold Tyrode's solution for transportation to the laboratory.² Alternatively, commercial cardioplegic solution, ringer lactate or standard ice-cold PBS are also suitable for histological applications as the ones described in this protocol.
3. Transfer the samples to 1.5 mL tube containing ice-cold fixative solution of 4% paraformaldehyde and incubate them for 1 h at 4°C or on ice.

⚠ **CRITICAL:** The fixation time and volume depend on the tissue size. This pipeline is optimized for biopsies collected using disposable 14 G tru-cut biopsy needles that render 5-to-10-mm long and approximately 2-mm thick ventricular tissue samples.

4. Remove the fixative solution and transfer the samples to 0.01% sodium azide-PBS at 4°C until embedded in paraffin blocks.

5. Carry out tissue dehydration and paraffin embedding with the Tissue-Tek Xpress x50 Tissue Processor System (Henry Schein, USA).
6. Mount tissue blocks using the paraffin embedding station EG1150H (Leica, Germany) and the HI1210 Water bath for paraffin sections (Leica, Germany). Other tissue sample processing and embedding procedures, preferentially automatized to minimize variability in tissue processing, are also applicable.
7. Section the tissue blocks with the microtome Shandon finesse 325 (Thermo Scientific, USA) to obtain 5- μm sections.

Note: Both a confocal and a two-photon microscope have the capability to capture high-quality optically sectioned images of tissue sections, even those with a thickness exceeding 100 μm . In samples with highly scattering structures, the crucial factor affecting image quality is the imaging depth rather than the actual thickness of the tissue section. Using the surface closest to the imaging objective lens always allows for the collection of high-quality images, even when dealing with thick tissue sections, as the light does not need to traverse the entire thickness of the section.

8. Mount the sections on microscope slides (MENZAA00008032E011, VWR, USA). Let the sections dry out 24 h before image acquisition with the microscope.

Note: Tissue sections should be allowed to dry after being mounted on the microscope to facilitate that the tissue better adheres to the slides. This drying is recommended regardless of the technique to be subsequently applied (e.g., label-free imaging or immunohistochemistry).

Image acquisition

⌚ **Timing:** 3 min for imaging 1 mm^2 tissue and around 20 min to set position and focus and save the imaged data

This section describes how to characterize collagen deposition in left ventricular tissue samples using Second Harmonic Generation (SHG) microscopy combined with two-photon excitation fluorescence (TPEF) microscopy to detect the autofluorescence of the myocardial tissue and the lipofuscin. We used a Zeiss LSM 880 microscope (Carl Zeiss, Germany) mounted on the rear port of an Axio Observer.Z1 stand. This analysis does not require any staining. Paraffined tissue sections mounted on microscope glass slides can be directly observed under the microscope.

9. The SHG and TPEF image acquisition procedure and microscope configuration are as follows:
 - a. Rotate a suitable objective lens into the imaging position (i.e., plan-apochromat 20 \times objective (NA 0.8, Carl Zeiss, Germany)).
 - b. Place a sample on the microscope sample holder. Locate and focus the sample using transmission or fluorescence imaging.

Note: Cellular and lipofuscin autofluorescence can be visualized using typical excitation and emission filters used for green (e.g., EGFP, Fluorescein) or red (e.g., mCherry, Alexa Fluor 555) fluorophores, respectively.

- c. Create a suitable light path to steer the femtosecond pulsed laser light to the sample.

Note: In our setup, laser light from the femtosecond pulsed laser (Mai Tai DeepSee, Spectra-Physics, CA, USA) is directed through an acousto-optic modulator into an LSM880 scanhead (Carl Zeiss, Germany). A 760 nm shortpass dichroic mirror (MBS 760+) is used to direct the laser light to the sample and to separate the laser light from the fluorescence and SHG signal.

- d. Activate three detectors to simultaneously detect the SHG signal, cellular autofluorescence and lipofuscin autofluorescence.

Note: The data can also be acquired sequentially in case three suitable detectors are not available.

- e. Adjust each detector channel to detect the optimal wavelength range:
- i. SHG signal: 380–420 nm.
 - ii. Cellular autofluorescence: 500–552 nm.
 - iii. Lipofuscin autofluorescence: 650–735 nm.

Note: In our setup, Ch1 (PMT), ChS1 (32 channel GaAsP array), and Ch2 (PMT) of the 34 channel QUASAR spectral detector unit of the Zeiss LSM 880 microscope are used for the SHG signal, cellular, and lipofuscin autofluorescence, respectively.

Note: The ZEISS QUASAR multichannel photomultiplier detection technology is based on a filter-free system that guides the desired wavelength range to the target detector using adjustable optical wedges and slider light stops. If using other microscopes, multiple emission filters can be suitable as long as they match the wavelength ranges listed in this protocol.

- f. Tune the femtosecond pulsed laser (Mai Tai DeepSee, Spectra-Physics, CA, USA) to a central wavelength of 810 nm and adjust the transmission through the acousto-optic modulator so that ~80 mW average power is focused on the sample through a plan-apochromat 20× objective (NA 0.8, Carl Zeiss, Germany).
- g. Adjust the acquisition parameters to acquire images with sufficient resolution and dynamic range.

Note: Preferentially use a bit depth of 16 bits. In our setup, a zoom factor of 1.3 is used to ensure a homogeneous illumination, and 1872 by 1872 pixels are acquired, thus resulting in a square pixel size of 170 nm by 170 nm.

- h. Fully open the pinhole(s) for each channel.
- i. Optimize the detection of each detector channel by adjusting the detector gain and offset.

Note: Use a range indicator lookup table while optimizing the detector settings to minimize data clipping by e.g., saturation. We employed the following detector settings:

- i. Ch1: detector gain 750, digital offset 256.
 - ii. ChS1: detector gain 680, digital offset 64.
 - iii. Ch2: detector gain 750, digital offset 256.
- j. Define a tilescan or mosaic image for samples larger than a single field-of-view by means of a rectangular grid or a bounding box for rectangular/square samples or irregular samples, respectively. Define sufficient overlap (i.e., 10%) between the different tiles to ensure proper stitching.

△ CRITICAL: Microscope acquisition settings need to be maintained between independent acquisition sessions so that all the tissue images are equally acquired.

Note: Higher quality images can be acquired using the non-descanned detectors of a confocal NLO microscope. In our setup, the conventional internal detectors are selected, as they allowed the acquisition of all three channels simultaneously, with good lateral and

axial overlap, significantly speeding up the acquisition process. To maximize the signal, the pinhole is fully opened, and optical sectioning is performed by the selective two-photon excitation process.

Image pre-processing

⌚ Timing: 5 min per sample

This section describes the image pre-processing for characterization of collagen features and quantification of lipofuscin content.

10. Image export and pre-processing:

- a. Zen Blue software is used to export 16-bit TIFF gray-scale images from the original czi files with each channel detected in a separate file. Images can be exported at once using batch processing. To keep the same parameter settings for the pre-processing of all the images, select Export image parameters for the first image > Copy parameters > Paste parameters in the other images (Figure 1).
- b. Open the three individual channels of each tissue section using ImageJ software.
- c. Delimit the tissue of interest of every channel with the tool “Polygon selection” and select “Edit > Clear outside” to clean isolated regions that should be discarded from the analysis due to e.g., fluorescence artifacts (Figure 2, see [troubleshooting problem 1](#)).
- d. Select “Image > Adjust > Brightness/Contrast” for automatic brightness scaling.³ Select each channel image and press “Auto” bottom once and then “Apply” (Figure 3A). Repeat this step with the other channels (Figure 3B).
- e. Save each of the adjusted images as a new 8-bit TIFF file.

⚠ **CRITICAL:** For robustness of the analysis, image pre-processing should preferably be applied to high-quality (16-bit) images.

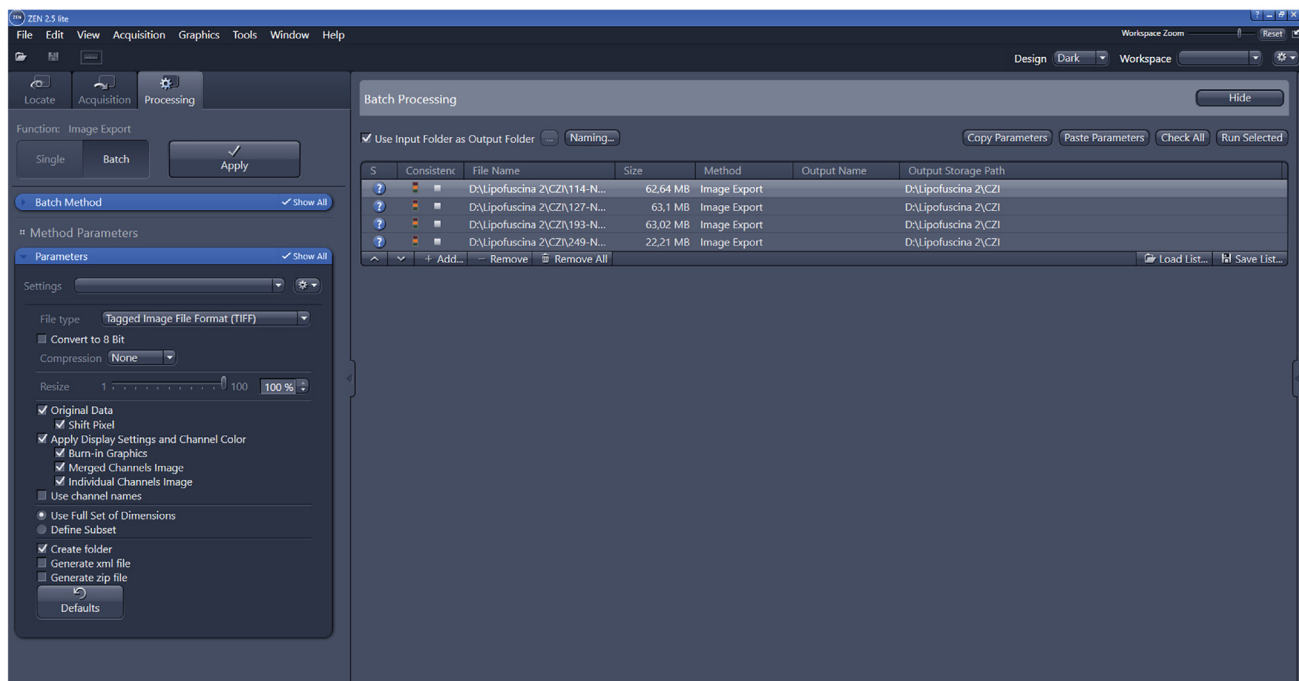


Figure 1. ZEN parameters for image export using batch configuration

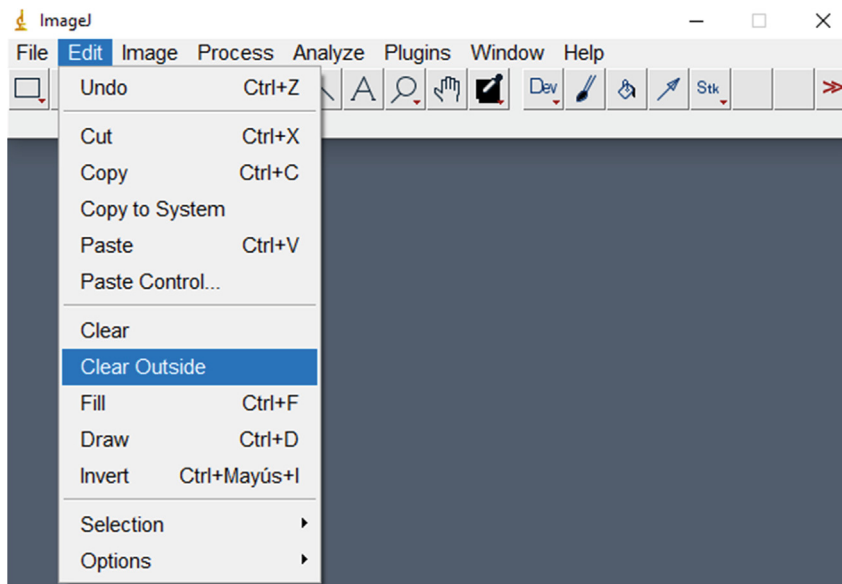


Figure 2. Screen view of Fiji edit menu to clean images before analysis

Collagen amount, aggregation, and spatial distribution analysis

⌚ Timing: 10–15 min per sample

This section describes the methods used to characterize collagen features in ventricular tissue samples.

11. Collagen amount quantification:

- a. Load each adjusted image saved as an 8-bit TIFF file and split it into its individual channels in grayscale.
- b. Apply a binarization filter to the gray-level images corresponding to the SHG signal or the autofluorescence signal from the myocardial tissue. Generate binary masks for each of the SHG signal, on the one side, and for the autofluorescence signal, on the other. These masks are referred to as *binary_SHG_channel_mask* and *binary_myocardial_tissue_mask*.

```
>binary_myocardial_tissue_mask = imbinarize(cellular_autofluorescence_channel,Thr1) (1)
>binary_shg_channel_mask = imbinarize(shg_signal_channel,Thr2) (2)
```

The MATLAB function “*imbinarize*” creates a binary image from a grayscale image by thresholding. The threshold luminance value is a numeric scalar with values in the range [0, 1]. The binarization threshold range that we used to generate binary masks was in the range 0.17–0.35 for the autofluorescence signal (*Thr1*) from which the myocardial tissue mask was extracted, and it was in the range 0.08–0.35 for the SHG signal (*Thr2*) from which the collagen mask was extracted.

- c. Fill empty spaces with less than 20 pixels in the myocardial tissue mask.

```
>myocardial_tissue_mask = imfill(binary_myocardial_tissue_mask,conn,'holes') (3)
```

The MATLAB function “*imfill*” fills holes in a binary image, in this case the *binary_myocardial_tissue_mask*. A hole is a set of background pixels that cannot be reached by filling in the background from the edge of the image. The input parameter *conn* specifies the pixel

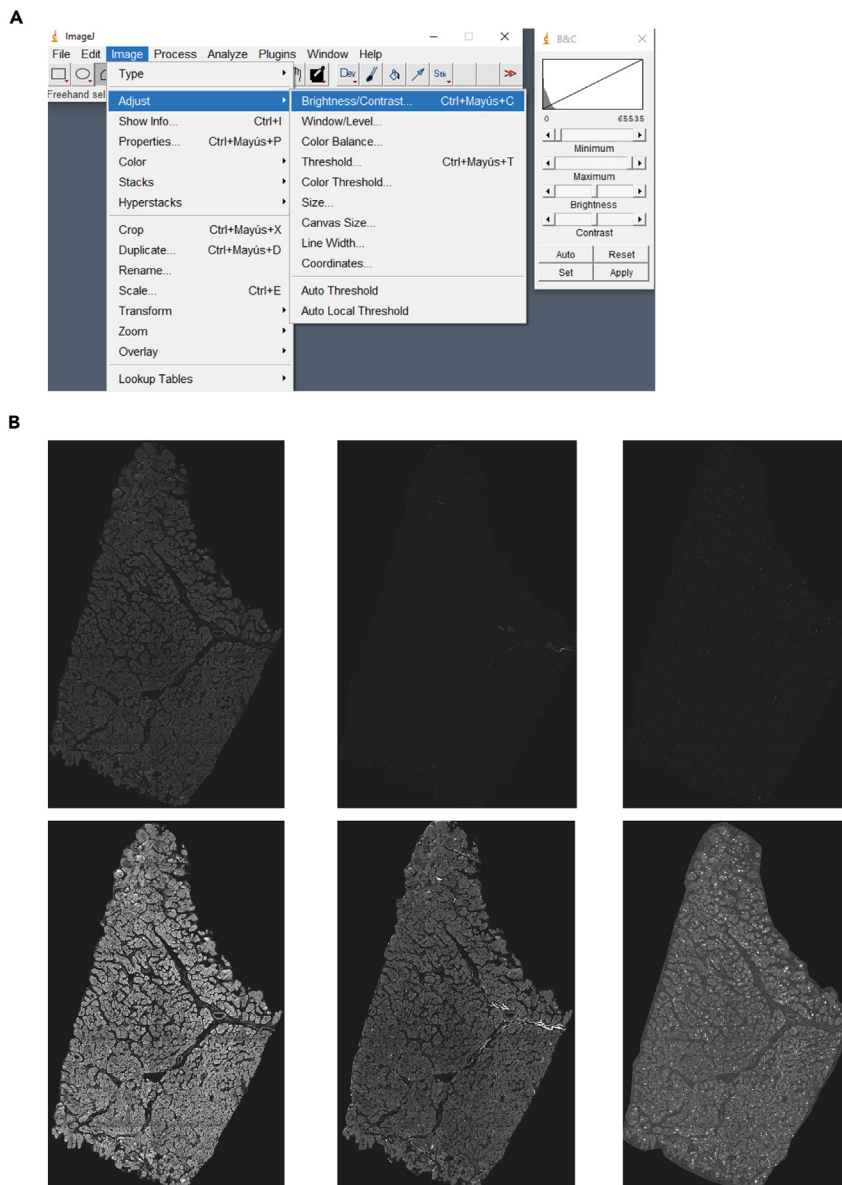


Figure 3. Fiji image menu to adjust image brightness

(A) Screen view of Fiji image.

(B) Original images (upper panel) and the corresponding images after brightness adjustment (lower panel) for autofluorescence signal from the myocardial tissue (left), SHG signal (middle) and lipofuscin (right).

connectivity. In our setup, 4-connected background neighbors are used, which means that the pixels are connected if their edges touch. The neighborhood of a pixel involves the adjacent pixels in the horizontal or vertical direction.

- d. Identify and remove isolated segments and/or artifacts in the SHG binary mask. In our setup, areas with less than 15 pixels in the SHG binary mask are discarded (defined as *new_binary_shg_signal_mask*).

```
>new_binary_shg_signal_mask = bwareaopen(binary_shg_signal_mask, P) (4)
```

The MATLAB function “*bwareaopen*” removes small objects from binary images. *P* defines the minimum number of pixels an area should have not to be removed.

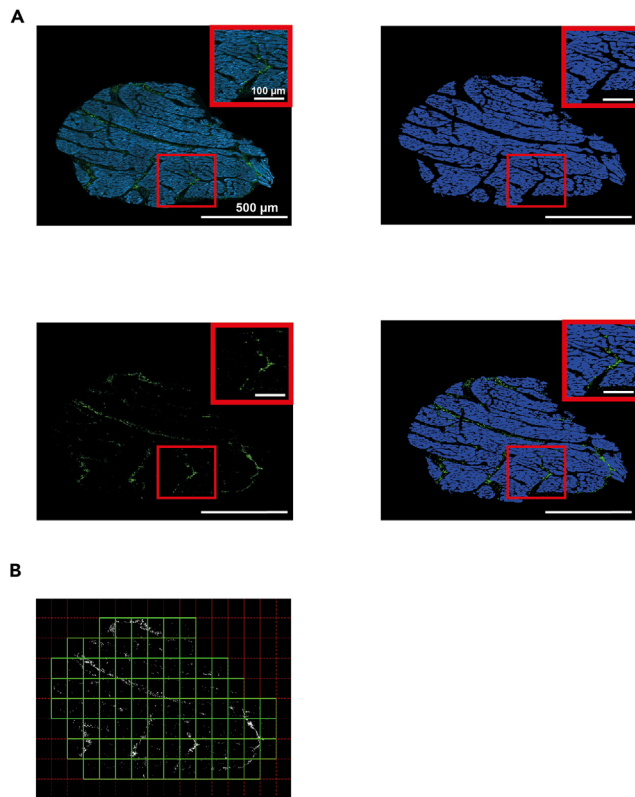


Figure 4. Collagen characterization from SHG images

(A) Unprocessed SHG image (green) and autofluorescence (blue) levels of a left ventricular tissue specimen (top panel left), extracted tissue mask obtained from the tissue autofluorescence signal (top panel right), collagen mask obtained by subtraction of autofluorescence to SHG signal (bottom panel left) and merge of collagen (green) and myocardial tissue (blue) masks (bottom panel right).

(B) Windowing of collagen mask to evaluate spatial distribution. Adapted from García-Mendivil et al.¹

- e. Separate the myosin and collagen signals in the SHG signal by considering that collagen is the part of the SHG signal that does not colocalize with the myocardial tissue mask (3). Based on this absence of colocalization, the collagen mask is obtained from the SHG channel mask (4) as follows (Figure 4A):

```
>rowNumber = size(new_binary_shg_signal_mask,1);           (5)
>columnNumber = size(new_binary_shg_signal_mask,2);
>collagen_mask = zeros(size(new_binary_shg_signal_mask));
>for i = 1 to rowNumber do
>for j = 1 to columnNumber do
>if new_binary_shg_signal_mask(i,j) = 1 and myocardial_tissue_mask(i,j) =0 then
>collagen_mask(i,j) = 1;
>end if
>end for
>end for
```

- f. Using the myocardial tissue mask (3) and the collagen mask (5), the percentage of collagen (P_c) is calculated as the number of activated pixels in the collagen mask (N_c) divided by the sum of activated pixels in the myocardial tissue (N_m) and the collagen masks:

$$P_c = \frac{N_c}{(N_c + N_m)} 100$$

where:

$$>N_c = \text{nnz}(\text{collagen_mask}); \quad (6)$$

$$>N_m = \text{nnz}(\text{myocardial_tissue_mask});$$

The MATLAB function "nnz" returns the number of nonzero elements in a specific matrix.

Note: The obtained binary masks are used in subsequent analyses.

12. Collagen aggregation analysis:

- a. Using the collagen binary masks, the global clustering degree (P_{sc}) is computed as the ratio between the number of collagen pixels surrounded by collagen pixels in a circle of 2-pixel radius (denoted by N_{sc}) and the total number of collagen pixels:

$$P_{sc} = \frac{N_{sc}}{N_c} 100$$

where:

$$>N_c = \text{nnz}(\text{collagen_mask});$$

$$>N_{sc} = \text{nnz}(\text{collagenPixelsSurrounded});$$

with the matrix collagen Pixels Surrounded being defined as follows:

```
>collagenPixelsSurrounded = zeros(size(collagen_mask));
>centroX_origen = radius+1;
>centroY_origen = radius+1;
>[columnsInImage rowsInImage] = meshgrid(centroX_origen - radius:centroX_origen
+ radius,centroY_origen - radius:centroY_origen+radius);
    >circleRadiusPixels = (rowsInImage - (radius+1))^2 + (columnsInImage - (radius+1))^2 ≤
radius2;
>[row_collagen_mask, column_collagen_mask] = find(collagen_mask==1);
>for i = 1 to length(row_collagen_mask) do
>if (row_collagen_mask(i) > radius) and (row_collagen_mask(i) <
    size(collagen_mask,1) - radius) and (column_collagen_mask(i) > radius) and
    (column_collagen_mask(i) < size(collagen_mask,2) - radius) then
>centerX = column_collagen_mask(i);
>centerY = row_collagen_mask(i);
>collagen_mask_window = collagen_mask (centerY - radius:centerY+
    radius,centerX - radius:centerX + radius);
>connected_pixels = collagen_mask_window.*circlePixelsMask;
>if (connected_pixels== circlePixelsMask) then
>collagenPixelsSurrounded (row_collagen_mask(i), column_collagen_mask(i)) = 1;
```

```
>end if
>end if
>end for
```

- b. Calculate a relative clustering degree as the product of percentages of collagen and clustering degree, which is expressed as per ten thousand ($\%_{100}$).
13. Collagen spatial distribution assessment:
 - a. Divide the collagen binary mask into subimages of 500×500 pixels (Figure 4B).
 - b. Include in the analysis only the subimages of the collagen binary mask with a minimum of 200 activated pixels.
 - c. For each of the subimages, compute the collage clustering degree as described in step 12.
 - d. Build the histogram of the collagen clustering degree from all subimages of a given image. Determine the collagen clustering median, calculated as the median of the clustering distribution statistical distribution, and the collagen clustering dispersion, calculated as the interquartile range of the clustering degree statistical distribution.

Note: In our setup, the following parameter values are determined empirically from our images: the 2-pixel radius for global collagen aggregation, the window of 500×500 pixels for the characterization of collagen spatial distribution, and the threshold of 200 pixels for subimage acceptance in collagen spatial distribution assessment. These three parameter values and the threshold values for the construction of the tissue and collagen binary masks should be adapted for each set of images being analyzed.

Note: The median and interquartile range of the collagen clustering statistical distribution is determined using MATLAB.

Lipofuscin quantification

⌚ Timing: 5–10 min per sample

This section describes the pipeline used for lipofuscin quantification in ventricular tissue samples.

14. Lipofuscin content quantification:
 - a. Apply a binarization filter to the gray-level image corresponding to the lipofuscin signal to generate a binary lipofuscin mask (Figure 5). The same MATLAB functions and Equations 1 and 2 are used, although in this case the threshold ($Thr3$) range is in the range 0.48–0.7.

```
>binary_lipofuscin_mask = imbinarize(lipofuscin_autofluorescence_channel, Thr3) (7)
```

- b. Compute the percentage of lipofuscin (P_l) as the number of activated pixels in the lipofuscin mask (N_l) divided by the activated pixels in the myocardial tissue mask (N_m):

$$P_l = \frac{N_l}{N_m} 100$$

where:

$$\begin{aligned} >N_l &= \text{nnz}(\text{binary_lipofuscin_mask}); \\ >N_m &= \text{nnz}(\text{myocardial_tissue_mask}); \end{aligned} \quad (8)$$

Note: The MATLAB functions “imbinarize” and “nnz” are described in step 11.

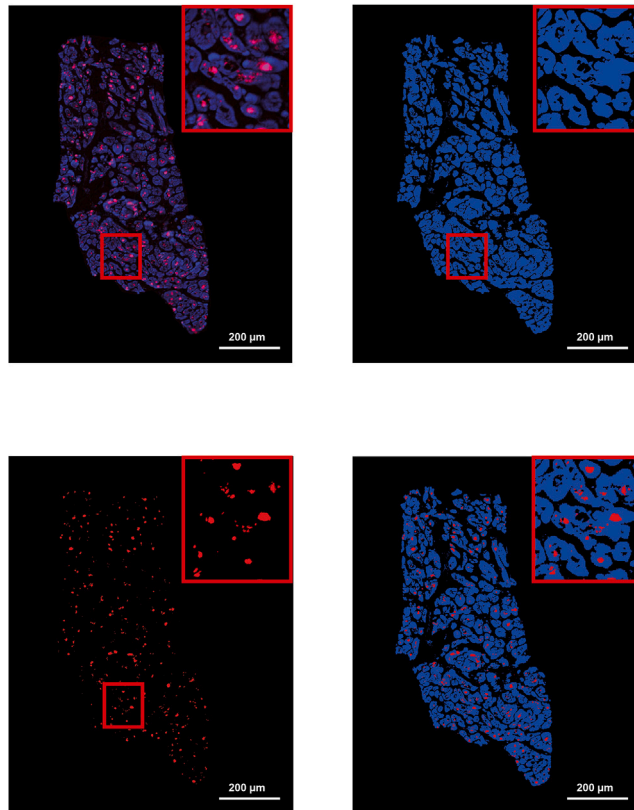


Figure 5. Quantification of lipofuscin accumulation by an automatic method

Unprocessed confocal microscopy image of a human left ventricular tissue section with lipofuscin (red) and tissue autofluorescence (blue) channels (top panel left), computed myocardial tissue mask (top panel right), computed lipofuscin mask (bottom panel left) and merge of lipofuscin and myocardial tissue masks (bottom panel right). Extracted from García-Mendivil et al.¹

EXPECTED OUTCOMES

Age is associated with the accumulation of interstitial fibrosis in the myocardium that alters the electromechanical function of the heart. Both collagen amount and spatial configuration have been reported to be relevant factors in impulse conduction and arrhythmia generation.^{4–7} However, the description of collagen characteristics additional to the amount has been scarcely investigated in humans. This protocol describes novel automatic processing methods that avoid discrepancies between observers and allow to characterize collagen remodeling, including new variables for spatial organization (aggregation and distribution across the tissue), and to quantify lipofuscin accumulation, a more accurate descriptor of cardiac functional state in relation to age. Due to the considerable interindividual variability in humans, the value of using biological age indicators, namely lipofuscin content in heart tissue, is highlighted. Although this protocol for automatic image analysis has been used to study collagen remodeling in human left ventricular samples, our pipeline can be applied to other fibrotic tissues and/or from other species. In the case of lipofuscin, its quantification can be evaluated from any tissue where it accumulates, such as the heart and the brain.

QUANTIFICATION AND STATISTICAL ANALYSIS

Statistical analysis between groups for collagen parameters and lipofuscin quantification can be performed using software like SPSS, MATLAB or GraphPad, among others. In the present study, statistical analyses are performed using MATLAB v2020b. The significance threshold is established at p -value = 0.05.

LIMITATIONS

The nature of automatic methods makes image processing objective, as opposed to those from manual methods, which are biased by the investigator performing. The protocol proposed here is optimized for automatic quantification of collagen features (content, aggregation and spatial organization) and of lipofuscin content using confocal images from human left ventricular tissue samples but could be extended to other tissues to generalize its use. Our image acquisition setup does not likely detect collagen III properly because of its low intensity SHG signal, but this would be systematic in all our samples.

TROUBLESHOOTING

Problem 1

Collagen analysis can be affected by the presence of perivascular fibrosis, which is not the interest of the present study, which is focused on the characterization of interstitial fibrosis in left ventricular tissues.

Potential solution

Image pre-processing should include a step where images are carefully checked before being included in the analysis and large vessels surrounded of perivascular fibrosis should be removed.

RESOURCE AVAILABILITY

Lead contact

Further information and requests for resources and reagents should be directed to and will be fulfilled by the lead contact, Dr. Laura Ordovás (lordovas@unizar.es).

Materials availability

This study did not generate new unique reagents.

Data and code availability

- All data reported in this paper will be shared by the [lead contact](#) upon request.
- Any additional information required to reanalyze the data reported in this paper is available from the [lead contact](#) upon request.

ACKNOWLEDGMENTS

This work was supported by Agencia Estatal de Investigación - Ministerio de Ciencia e Innovación (Spain) (PID2019-105674RB-I00, PID2022-140556OB-I00, TED2021-130459B-I00, and PID2022-139859OB-I00 funded by MCIN/10.13039//501100011033 and "ERDF A way of making Europe"), Gobierno de Aragón (LMP94_21 and LMP128_21 and BSICoS group T39_23R), and the European Research Council through G.A. (638284). L.G.-M. was supported by a predoctoral fellowship from the Departamento de Ciencia, Universidad y Sociedad del Conocimiento from the Gobierno de Aragón 2016–2020 co-funded by Programa Operativo del Fondo Social Europeo Aragón (C150/2016), EMBO Short-Term Fellowships (7710), and Ibercaja-CAI Estancias de Investigación (IT18/18). The authors would like to acknowledge the Cardiovascular Surgery Department of Miguel Servet University Hospital (Zaragoza, Spain) for providing human left ventricular samples. We also wish to thank the Anatomic Pathology Core Unit of Aragon Health Sciences Institute (IACS) for their contribution to histological processing. The graphical abstract was partly generated using Servier Medical Art, provided by Servier, licensed under a Creative Commons Attribution 3.0 Unported license and Freepik (https://www.freepik.com/free-vector/computer-with-keyboard-mouse-cartoon-style-isolated_10004861.htm#query=cartoon%20computer&position=21&from_view=keyword&track=ais)> Image by brgfx on Freepik).

AUTHOR CONTRIBUTIONS

L.G.-M., M.P.-Z., L.O., and E.P. conceived the study. L.O. and E.P. supervised the study. L.G.-M., M.P.-Z., and S.D. performed the experiments and analyzed the data. L.G.-M. wrote the manuscript

with contributions from M.P.-Z., L.O., and E.P., and all the authors carefully reviewed the data and the manuscript.

DECLARATION OF INTERESTS

The authors declare no competing interests.

REFERENCES

1. García-Mendivil, L., Pérez-Zabalza, M., Mountris, K., Duwé, S., Smisdrom, N., Pérez, M., Luján, L., Wolfs, E., Driesen, R.B., Vallejo-Gil, J.M., et al. (2022). Analysis of age-related left ventricular collagen remodeling in living donors: Implications in arrhythmogenesis. *iScience* 25, 103822.
2. Oliván-Viguera, A., Pérez-Zabalza, M., García-Mendivil, L., Mountris, K.A., Orós-Rodrigo, S., Ramos-Marquès, E., Vallejo-Gil, J.M., Fresneda-Roldán, P.C., Fañanás-Mastral, J., Vázquez-Sancho, M., et al. (2020). Minimally invasive system to reliably characterize ventricular electrophysiology from living donors. *Sci. Rep.* 10, 19941.
3. Schneider, C.A., Rasband, W.S., and Eliceiri, K.W. (2012). NIH Image to ImageJ: 25 years of image analysis. *Nat. Methods* 9, 671–675.
4. de Bakker, J.M., van Capelle, F.J., Janse, M.J., Tasseron, S., Vermeulen, J.T., de Jonge, N., and Lahpor, J.R. (1993). Slow conduction in the infarcted human heart. "Zigzag" course of activation. *Circulation* 88, 915–926.
5. de Jong, S., van Veen, T.A.B., van Rijen, H.V.M., and de Bakker, J.M.T. (2011). Fibrosis and Cardiac Arrhythmias. *J. Cardiovasc. Pharmacol.* 57, 630–638.
6. Kawara, T., Derksen, R., de Groot, J.R., Coronel, R., Tasseron, S., Linnenbank, A.C., Hauer, R.N., Kirkels, H., Janse, M.J., and de Bakker, J.M. (2001). Activation Delay After Premature Stimulation in Chronically Diseased Human Myocardium Relates to the Architecture of Interstitial Fibrosis. *Circulation* 104, 3069–3075.
7. Kazbanov, I.V., ten Tusscher, K.H.W.J., and Panfilov, A.V. (2016). Effects of Heterogeneous Diffuse Fibrosis on Arrhythmia Dynamics and Mechanism. *Sci. Rep.* 6, 20835.